

Local structure and bonding of Er in GaN: A contrast with Er in Si

P. H. Citrin and P. A. Northrup
Bell Labs, Lucent Technologies, Murray Hill, New Jersey 07974

R. Birkhahn and A. J. Steckl
University of Cincinnati, Nanoelectronics Laboratory, Cincinnati, Ohio 45221

(Received 13 January 2000; accepted for publication 21 March 2000)

X-ray absorption measurements from relatively high concentrations of Er (>0.1 at. %) doped in GaN films show that Er occupies the Ga site with an unprecedentedly short Er–N bond length. Electroluminescence intensities from these GaN:Er films correlate with the concentration of Er atoms that replace Ga, not with the abundantly present O impurities in the host. Simple chemical concepts are used to explain each of these results and their striking difference from those obtained for Er-doped Si. © 2000 American Institute of Physics. [S0003-6951(00)03320-9]

The $1.54 \mu\text{m}$ luminescence observed in Er-doped semiconductors has generated much interest due to its potential utility in optoelectronics.^{1,2} The intensity of such near-infrared (IR) luminescence in Er-doped Si,¹ for example, depends strongly on temperature, with significant quenching at 300 K. The intensity also depends sensitively on the amount of O present for reasons traceable to the local structure of Er.³ Specifically, in a Si host that is O poor, Er occupies neither substitutional nor interstitial sites, but instead breaks apart the Si bonds and forms optically inactive defects/precipitates resembling erbium silicide.^{4,5} In a Si host that is O rich, Er preferentially getters the O and forms soluble, optically active defects resembling erbium oxide. The amount of O in Si thus affects not only the optical activity of Er but the amount of Er that can be incorporated in Si by avoiding the formation of Er silicide precipitates.

Gallium nitride has recently become the focus of studying Er and other rare-earth (RE) dopants for several reasons,² among them being the absence of near-IR emission quenching and the presence of strong visible emission peaks at 300 K.⁶ In this letter, electroluminescence and x-ray absorption structural measurements from Er-doped GaN films are reported, which not only are unaffected by the amount of O present but contrast dramatically with those of Si:Er in almost every other way. Our findings are explained here in simple chemical terms and have important implications on future studies of GaN doped with Er and other RE metals.

Following procedures described elsewhere,⁷ GaN:Er films were grown by molecular beam epitaxy (MBE) onto 2 in. Si substrates and studied as a function of Ga cell temperature, i.e., separate substrates were prepared for each temperature.⁸ The Er concentration in these samples, determined with secondary ion mass spectrometry (SIMS), ranges from ~ 0.15 to ~ 0.3 at. %. Room temperature Er electroluminescence (EL) was measured peaking in the visible (green) at 537 nm (${}^2H_{11/2} \rightarrow {}^4I_{15/2}$) and 558 nm (${}^4S_{3/2} \rightarrow {}^4I_{15/2}$) and in the near-IR at $\sim 1.54 \mu\text{m}$ (${}^4I_{13/2} \rightarrow {}^4I_{15/2}$). Peak EL intensities in the visible (and less so in the near-IR) were found to vary with Ga cell temperature, see Fig. 1. For clarity, only variations in 558 nm EL are plotted. In view of the reported role played by O in affecting Er emission intensities in GaN:Er,⁹ O concentrations (measured with SIMS) were considered as a possible source for these variations.

High, and nonsystematically, widely varying O concentrations for the individually prepared samples were found, as shown in Fig. 1. However, no correlation of these values with Er luminescence intensity in either the visible or near-IR regions was observed.

Fluorescence-detection Er L_3 -edge extended x-ray absorption fine structure (EXAFS) measurements from samples cooled to <15 K (to minimize thermal disorder effects¹⁰) were obtained at the National Synchrotron Light Source (NSLS) using the Bell Laboratories X15B beamline. Figure 2 shows Fourier transformed (FT) EXAFS data from the GaN:Er sample exhibiting the strongest Er visible luminescence. The FT peaks correspond to coordination shells surrounding Er at distances R' (uncorrected for phase shifts¹⁰) and typify the Er local structure, which is identified in Fig. 2 by comparison with the known peak assignments in the Ga K -edge EXAFS data from GaN.¹¹ It is clear that Er substitutionally occupies the Ga site. The similarity in relative peak FT intensities between the first-shell N and second-shell Ga atoms provides direct evidence that this local Er structure is highly ordered.¹⁰ Significantly, edge-normalized FT data (not shown) from the other GaN:Er samples exhibiting weaker visible Er luminescence display identical FT peak positions but with lower absolute peak intensities, indicating that in these other samples a smaller fraction of Er atoms occupies Ga sites.¹² The combined FT magnitudes of the peaks at

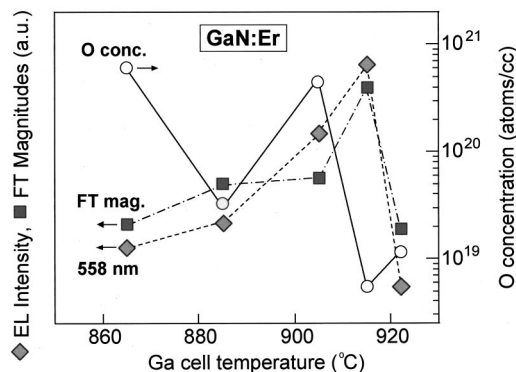


FIG. 1. EL peak intensities at 558 nm (linear scale) and oxygen concentrations (log scale) measured from GaN:Er samples grown with different Ga cell temperatures. Also plotted are the magnitudes of FT EXAFS data from the FT peaks at $R' \approx 1.8$ and 3.0 \AA (see Fig. 2).

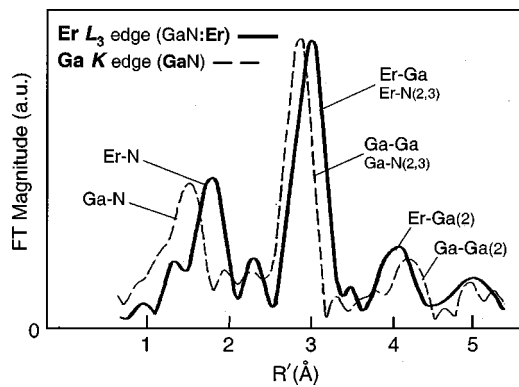


FIG. 2. FT Er L_3 -edge EXAFS data from the GaN:Er sample grown with a Ga cell temperature of 915 °C, and Ga K -edge data from GaN (Ref. 11). Data were normalized at the FT peak at ~ 3 Å. The R' values do not include corrections for phase shifts, which vary with edge (L_3, K), absorbing atom (Er, Ga), and backscattering atom (N, Ga).

$R' \approx 1.8$ and 3.0 Å from these other samples are included in Fig. 1, establishing that the Er visible EL intensities correlate with the concentration of dopant Er atoms that replace Ga, not with the concentration of impurity O atoms.

More detailed analyses using standard procedures^{10,13} reveal that the first-neighbor Er–N bond in GaN:Er is 2.17 ± 0.02 Å, or ~ 0.22 Å longer than the corresponding Ga–N bond length in GaN. (The Er–Ga distance at 3.26 ± 0.03 Å is ≤ 0.1 Å longer than that for Ga–Ga.) This increase in bond length, unsurprising because Er is obviously larger than Ga, belies the unusual nature of this Er–N bond. It is the shortest Er–N bond length measured, shorter by ~ 0.25 Å than in ErN and even shorter by ~ 0.05 Å than in organometallic amide complexes.¹⁴ In fact, it appears to be the shortest measured Er bond length in a compound of any kind.

Why is the Er–N bond length in GaN:Er so short? Why does Er, despite its larger size, occupy a lattice site in GaN but not in Si? Why is O, despite its abundance, not gettered by Er in GaN but gettered by Er in Si? We argue that each of these questions is related to the chemical nature of and difference between the Er–N and Er–Si bonds in their hosts.

Table I lists relevant Er-containing systems and corresponding coordination numbers and bond lengths, along with those from GaN and Si. Also listed are values of first-neighbor electronegativity differences,¹⁵ which are useful parameters for qualitatively gauging relative degrees of

TABLE I. Bond length and strength as a function of number and type of first-neighbor atom.

System	Bond	C.N.	R (Å)	Δ_{electr}^a	ε_b (eV) ^b
Er	Er–Er	12 ^c	3.51 ^c	0	0.7 ^d
ErSi _{1.7}	Er–Si	10 ^c	2.92 ^{c,e}	0.7	0.9
ErN	Er–N	6	2.42	2.0	2.2
Er ₂ O ₃	Er–O	6 ^c	2.27 ^c	2.4	3.0
GaN:Er	Er–N	4	2.17 ^f	2.0	>2.2
Si	Si–Si	4	2.35	0	2.3 ^d
GaN	Ga–N	4	1.95	1.3	2.2

^aElectronegativity difference, from Ref. 15.

^bCohesive energy per bond for Er(III) and host (Si, Ga) atoms.

^cAverage coordination numbers and bond lengths quoted.

^dNumber of bonds per unit cell is 6 in Er and 2 in Si.

^eSee Ref. 5.

^fThis work.

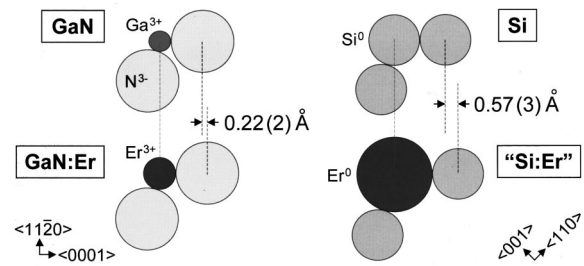


FIG. 3. View in the $\langle 110 \rangle$ plane of nearest-neighbor distances from systems with the same coordination but different chemical bonding character: Si–Si (covalent), Si–Er (metallic), Ga–N (polar covalent) and Er–N (ionic). The measured bond length difference and structure for GaN:Er come from this work. The Si:Er system shows the structure predicted for substitutional Er using the Er–Si distance measured from Ref. 5. Indicated crystallographic directions are referenced to unit cells of GaN (wurtzite) and Si (diamond).

covalent/ionic bonding. These values show that the Er–Si bonds in metallic ErSi_{1.7}, which closely resemble those of Er in Si both in number and length,^{3,5} are only somewhat less covalent than the purely covalent and metallic bonds in semiconducting Si and Er metal. This makes it appropriate to consider the size and bonding of Er in GaN as being similar to that of neutral trivalent Er⁰ in its metal-atom configuration,¹⁶ i.e., Er(III) $4f^{11}6s^25d^1$.¹⁷ Indeed, summing the radii of Er metal (1.755 Å) and of Si (1.175 Å) gives an Er–Si bond length in excellent agreement with that found for ErSi_{1.7} (see Table I) and for Er in Si.^{3,5} By contrast, the Ga–N bonds in almost insulating GaN are relatively polar, lying closer to the ionic Er–N and Er–O bonds in the insulating salts ErN and Er₂O₃. The more ionic Er–N bonds in GaN:Er make it appropriate to consider the size and bonding of Er in GaN as being similar to that of Er³⁺ ion in ErN,¹⁶ i.e., Er(III) $4f^{11}$. Summing the ionic radii for six-fold coordinated Er³⁺ (0.89 Å) and N³⁻ (1.46 Å)¹⁸ slightly underestimates the Er–N distance in ErN but overestimates it more in GaN:Er. Correcting these radii for their lower four-fold coordination,¹⁹ however, *viz.*, 0.78 and 1.44 Å, brings their sum into much closer agreement with experiment.

Figure 3 contrasts how these different Er–N and Er–Si bonds affect the local environment assuming Er occupies the same substitutional site in Si as in GaN (Er in a T_d interstitial Si site would have the same Er–Si distance and a similar effect). The increase in volume needed to accommodate Er in the hypothetical “Si:Er” system is seen to be considerable, ~ 2.5 times greater than that for Er in GaN. Such an unphysically large Si expansion explains, in part, why Er occupation of Si lattice sites (or interstices) is so unfavorable.

Additional insight into this question, as well as the others posed earlier, is gained by considering the relative energy costs of breaking and forming bonds between Er, the host atoms, and O. The bond energy, ε_b , or equivalently, cohesive energy per bond, is listed for the relevant systems in Table I. This quantity is calculated for solid M_aX_b by taking its cohesive energy per neutral free M atom (with the atom in its final, solid-state electronic configuration¹⁷) and dividing that energy by the number of M – X bonds in the unit cell.²⁰

The ε_b values are highly informative. First, despite covalent versus ionic bonding differences between the host atoms themselves, $\varepsilon_b(\text{Si–Si}) \approx \varepsilon_b(\text{Ga–N})$. This means that in the Er doping process, there are negligible energy differences

associated with breaking Si–Si vs Ga–N bonds, regardless of how many such bonds are broken to accommodate Er. Second, because of bonding differences between Er and the host atoms, $\epsilon_b(\text{Er–Si}) \ll \epsilon_b(\text{Er–N})$. This means that our views about distinctions in size and bonding character for Er⁰ in Si vs Er³⁺ in GaN,¹⁶ discussed earlier and highlighted in Fig. 3, are well corroborated by the different Er–Si and Er–N bond strengths. Third, because of ionic bonding similarities between ErN and GaN, $\epsilon_b(\text{Er–N}) \approx \epsilon_b(\text{Ga–N})$; because of metallic versus covalent bonding differences between ErSi_{1.7} and Si, $\epsilon_b(\text{Er–Si}) \ll \epsilon_b(\text{Si–Si})$. This means that the slightly larger size of four-fold coordinated Er³⁺ vs Ga³⁺ is offset by the lower electronegativity of Er,¹⁶ making it energetically inexpensive for Er to substitute for Ga in GaN.²¹ Conversely, the much larger size of Er⁰ vs Si makes it energetically prohibitive to occupy a four-fold coordinated Si site.²² Instead, by breaking apart the Si host bonds, increasing the Er coordination to 10, and reforming new Si–Si bonds—all of which is found in the Si:Er defects resembling ErSi_{1.7}^{3,5}—the energies become favorable.

The values of ϵ_b in Table I also have bearing on the questions of O gettering and the Er–N bond length in GaN:Er. Since $\epsilon_b(\text{Er–O}) > \epsilon_b(\text{Er–N}) \gg \epsilon_b(\text{Er–Si})$, it follows that it should be easier for O to be gettered by Er when it is in Si rather than in GaN. In fact, the relative insensitivity of Er to O in GaN:Er is related to the short Er–N bond length. We stated earlier that because $\epsilon_b(\text{Er–N}) \approx \epsilon_b(\text{Ga–N})$, it is energetically inexpensive to substitute Er for Ga in GaN, but the $\epsilon_b(\text{Er–N})$ value used in Table I is derived from six-fold coordinated Er in ErN. Since coordination number and bond length for a given atom are both inversely related to bond strength, the unusually short Er–N bond in GaN:Er is obviously coupled with the unusually low four-fold coordination of Er, and therefore $\epsilon_b(\text{Er–N, GaN:Er}) > \epsilon_b(\text{Er–N, ErN})$. This, in turn, implies that it should be even more energetically favorable for Er to replace Ga in GaN, and for Er in GaN:Er not to getter O.

These findings have several practical implications. Occupying the Ga site in GaN, which has no inversion symmetry, allows for otherwise forbidden Er 4*f* intrashell transitions. This means that increasing the Er luminescence intensity in GaN:Er should involve increasing the number of substitutional Er atoms, as observed. We have shown above that replacing Er for Ga is influenced less by energetics than by the size of the strain field surrounding Er. Our EXAFS data indicate that local lattice displacements are negligible beyond ~ 5 Å from Er, which translates into an average Er–Er separation of ~ 10 Å, or an effective Er concentration of $\sim 10^{21}$ atoms/cm³ (~ 1 at. %). This is more than four orders of magnitude greater than that for Er in O-poor Si.²² The substitution of Er for Ga in GaN will, of course, also depend on other factors such as growth conditions and doping methods (e.g., MBE versus implantation), but the presence of O should not be one of them. Our understanding of how Er luminescence can be optimized from GaN:Er clearly extends to other trivalent rare earth metals, whose size and chemical bonding properties are all comparable.

In summary, we have shown that Er replaces Ga in GaN, yielding unusually short Er–N bonds due to the low four-fold coordination and ionic character of Er. Similarly simple

concepts are used to explain why such substitution is energetically favorable, why Er in GaN is insensitive to O in the host, and why this behavior is so different for Er in Si. That the optically favorable Ga site is also amenable to substitution with relatively high concentrations of rare earth dopants makes GaN an ideal material for use in optoelectronics.

The authors thank A. Frenkel, W. J. Evans, and B. Batlogg for helpful discussions. The x-ray absorption measurements were performed at the NSLS, Brookhaven National Laboratory, which is supported by the DOE, Division of Materials Science and Division of Chemical Sciences. The research at Cincinnati is supported in part by BMDO/ARO.

¹ See, e.g., J. Michel, L. V. C. Assali, M. T. Morse, and L. C. Kimerling, *Semicond. Semimet.* **49**, 111 (1998).

² See, e.g., A. J. Steckl and J. M. Zavada, *Mater. Res. Bull.* **24**, 33 (1999).

³ D. L. Adler, D. Jacobson, D. J. Eaglesham, M. Marcus, J. Benton, J. M. Poate, and P. H. Citrin, *Appl. Phys. Lett.* **61**, 2181 (1992).

⁴ R. Sema, M. Lohmeier, P. M. Zagwijn, and A. Polman, *Appl. Phys. Lett.* **66**, 1385 (1995).

⁵ P. H. Citrin, D. R. Hamann, P. Northrup, D. Jacobson, J. Michel, T. Chen, M. Platero, and L. C. Kimerling (unpublished).

⁶ A. J. Steckl and R. Birkhahn, *Appl. Phys. Lett.* **73**, 1700 (1998).

⁷ M. Garter, J. Scofield, R. Birkhahn, and A. J. Steckl, *Appl. Phys. Lett.* **74**, 182 (1999).

⁸ R. Birkhahn, J. Heikenfeld, M. Garter, D. S. Lee, A. J. Steckl, K. Lorenz, R. Vianden, M. F. da Silva, J. C. Soares, E. Alves, A. Saleh, P. A. Northrup, and P. H. Citrin (unpublished).

⁹ J. D. MacKenzie, C. R. Abernathy, S. J. Pearton, U. Hömmerich, J. T. Seo, R. G. Wilson, and J. M. Zavada, *Appl. Phys. Lett.* **72**, 2710 (1998).

¹⁰ P. A. Lee, P. H. Citrin, P. Eisenberger, and B. M. Kincaid, *Rev. Mod. Phys.* **53**, 769 (1981).

¹¹ K. E. Miyano, J. C. Woicik, L. H. Robins, C. E. Bouldin, and D. K. Wickenden, *Appl. Phys. Lett.* **70**, 2108 (1997).

¹² EXAFS from Er in other configurations destructively interfere and lead to reduced amplitudes.

¹³ Consistent results were obtained using phase shifts and scattering amplitudes determined empirically from model compounds or theoretically from FEFF6, cf., S. Zabinsky, J. Rehr, A. Ankoudinov, R. Albers, and M. Eller, *Phys. Rev. B* **52**, 2995 (1995).

¹⁴ R. Anwander, *Top. Curr. Chem.* **179**, 33 (1996).

¹⁵ G. Busch and H. Schade, *Vorlesungen Über Festkörperphysik* (Birkhäuser Verlag, Basel, 1973).

¹⁶ The electronegativity of Er, as well as the sizes of Er⁰ and Er³⁺, are comparable to those of Na⁰ and Na¹⁺ or Ca⁰ and Ca²⁺.

¹⁷ Trivalent Er(III), which is its configuration in the solid state, simply means there are three available valence electrons rather than the two available in the divalent free atom, Er(II) 4*f*¹²6*s*².

¹⁸ R. D. Shannon, *Acta Crystallogr., Sect. A: Cryst. Phys., Diffr., Theor. Gen. Crystallogr.* **32**, 751 (1976).

¹⁹ The \sim linearly varying Er³⁺ radii with coordination from Ref. 18 are extrapolated, while the N³⁻ radii are assumed to vary linearly as those for O²⁻.

²⁰ Consider, e.g., the 6 Er–O bonds in Er₂O₃: $\epsilon_b = (1/6)E'_{\text{coh}}$; $E'_{\text{coh}} = (1/2)E_{\text{coh}}$; $E_{\text{coh}} = 2\text{Er}^{\text{III}}(g) + 3\text{O}(g) = \Delta H_f^0 + 2\Delta H'_{\text{vap}}[\text{Er}^{\text{III}}(m)] + (3/2)\Delta H_{\text{dissoc}}(\text{O}_2)$; $\Delta H'_{\text{vap}}[\text{Er}^{\text{III}}(m)] = \Delta H_{\text{vap}}[\text{Er}(m)] + E_{\text{config}}$; $E_{\text{config}} = E[\text{Er}^{\text{III}}(g)] - E[\text{Er}^{\text{II}}(g)]$. Standard heats of formation, vaporization, and dissociation are from common sources, except ΔH_f^0 for ErN and ErSi_{1.7} which are, respectively, from J. Kordis and K. Gingerich, *J. Nucl. Mater.* **66**, 197 (1977); R. Pretorius, T. Marais, and C. Theron, *Mater. Sci. Eng.* **10**, 1 (1993). The Er free-atom configuration energy, E_{config} , is from A. Fujimori, M. Grioni, and J. Weaver, *Phys. Rev. B* **33**, 726 (1986), as is the contribution to E_{coh} from the 2.5 Si–Si bonds in ErSi_{1.7} (it is subtracted from E_{coh} to isolate the contribution of Er–Si bonds).

²¹ The similar Er–N and Ga–N bond energies also explain why the local Er structure, i.e., the EXAFS in Fig. 2, is so highly ordered.

²² The low solubility observed for Er in O-poor Si, $< 5 \times 10^{16}$ cm⁻³, cf., Ref. 1, is consistent with the low Er–Si bond energy.